Current Optics and Photonics
Vol. 4, No. 6, December 2020, pp. 509-515

ISSN: 2508-7266(Print) / ISSN: 2508-7274(Online)
DOI: https://doi.org/10.3807/COPP.2020.4.6.509

Fabrication Tolerance of InGaAsP/InP-Air-Aperture Micropillar Cavities as 1.55-μm Quantum Dot Single-Photon Sources

Shuai Huang[1,2], Xiumin Xie[1], Qiang Xu[1], Xinhua Zhao[1], Guangwei Deng[2], Qiang Zhou[2]*, You Wang[1,2], and Hai-Zhi Song[1,2]**

[1]*Southwest Institute of Technical Physics, Chengdu 610041, China*
[2]*Institute of Fundamental and Frontier Sciences, University of Electronic Science and Technology of China, Chengdu 610054, China*

(Received July 13, 2020 : revised September 6, 2020 : accepted October 14, 2020)

A practical single photon source for fiber-based quantum information processing is still lacking. As a possible 1.55-μm quantum-dot single photon source, an InGaAsP/InP-air-aperture micropillar cavity is investigated in terms of fabrication tolerance. By properly modeling the processing uncertainty in layer thickness, layer diameter, surface roughness and the cavity shape distortion, the fabrication imperfection effects on the cavity quality are simulated using a finite-difference time-domain method. It turns out that, the cavity quality is not significantly changing with the processing precision, indicating the robustness against the imperfection of the fabrication processing. Under thickness error of ±2 nm, diameter uncertainty of ±2%, surface roughness of ±2.5 nm, and sidewall inclination of 0.5°, which are all readily available in current material and device fabrication techniques, the cavity quality remains good enough to form highly efficient and coherent 1.55-μm single photon sources. It is thus implied that a quantum dot contained InGaAsP/InP-air-aperture micropillar cavity is prospectively a practical candidate for single photon sources applied in a fiber-based quantum information network.

Keywords : Microcavity, Single photon source, Quantum dot, Telecommunication band, Fabrication tolerance
OCIS codes : (080.2208) Fabrication, tolerancing; (140.3945) Microcavities; (220.4000) Microstructure fabrication; (250.5590) Quantum-well, -wire and -dot devices; (270.5585) Quantum information and processing

I. INTRODUCTION

Microcavities containing semiconductor quantum dots (QDs) serve as efficient [1, 2] and even coherent single photon sources (SPSs) [3, 4]. Owing to the high coupling efficiency to fiber [5] and the suitability for electrical driving [6], micropillar cavities are advantageous for fiber-based quantum information processing. In telecommunication-band quantum networks, 1.55-μm InAs/InP QDs contained micropillar cavities are strongly required as SPSs [7], but such an SPS is not practically available yet. The main reason is that the low refractive-index contrast in materials monolithically grown on InP [8] makes it difficult to fabricate efficient micropillar cavities composed of InP/InGaAsP or AlInGaAs/AlInAs distributed Bragg reflectors (DBRs). Hybrid microcavities, such as Ta_2O_5/SiO_2-InP micropillars [9] and Si/SiO_2-InP micropillars [10, 11], were thus designed for 1.55 μm QD-SPS, but their fabrication needs complicated processing techniques, which are subject to failure because of the difficulty to match different material systems and compress interface defects. Recently, we proposed a design of InGaAsP/InP-air-aperture micropillar cavity [12], which is more advantageous than before because it needs only monolithic fabrication processing,

*Corresponding author: zhouqiang@uestc.edu.cn, ORCID 0000-0001-7099-1995
**Corresponding author: hzsong1296@163.com, ORCID 0000-0003-1538-2470
Color versions of one or more of the figures in this paper are available online.

and avoids damage near the light source caused by thin active layer and the mismatching processing between different materials. Ideal structures of this micropillar cavity satisfy well the requirements of efficient and coherent SPS at 1.55 μm. However, the real cavity structure may be distant from the ideal one so that a practically available cavity might not be as suitable as expected [13, 14]. It is thus necessary to further study the fabrication tolerance of this cavity, i.e., whether a practically accessible structure is qualified to serve as an efficient and coherent SPS. In this work, we investigate the property of the InGaAsP/InP-air-aperture micropillar cavity depending on the layer size fluctuation, surface roughness and shape distortion, and confirm the robustness of this cavity against fabrication uncertainty.

II. IDEAL CAVITY AND METHOD

The fundamental cavity structure is schematically demonstrated by the upper inset in Fig. 1. The pillar structure consists of disk shaped (in XY plane) and coaxially set (in Z direction) InGaAsP and InP layers with different diameters D and d (termed outer and inner diameters hereafter, respectively), alternatively stacked on an InP substrate. The small-size InP layers are surrounded by peripheral air-gaps, or so-called air-apertures. The top and bottom parts of the pillar are conventional DBRs composed of periodical InGaAsP and InP-air-aperture layers. The thickness of each InP layer in the DBRs is set as $t_1 = \lambda_B/4$, where λ_B is the Bragg wavelength around 1.55 μm; while each InGaAsP layer in the DBRs is set quarter-wavelength thick as $t_2 = \lambda_B/(4n_2)$, where n_2 is the refractive index of InGaAsP. In between the conventional DBRs, there are incorporated more InGaAsP/InP-air-aperture segments (pairs) as adiabatic DBRs on both the top and bottom sides. The adiabatic DBRs have linearly decreasing layer thicknesses $t_{1i} = t_1(1-\rho(2i-1))$ for InP and $t_{2i} = t_2(1-2\rho i)$ for InGaAsP, where i is the segment number and ρ the changing rate of layer thickness. In between the adiabatic DBRs, an InP layer is inserted as the central spacer with thickness $t_0 = t_1(1-2\rho N)$, where N is the total segment number in one side adiabatic DBR. An InAs/InP QD is set in this layer as the light-emitting source.

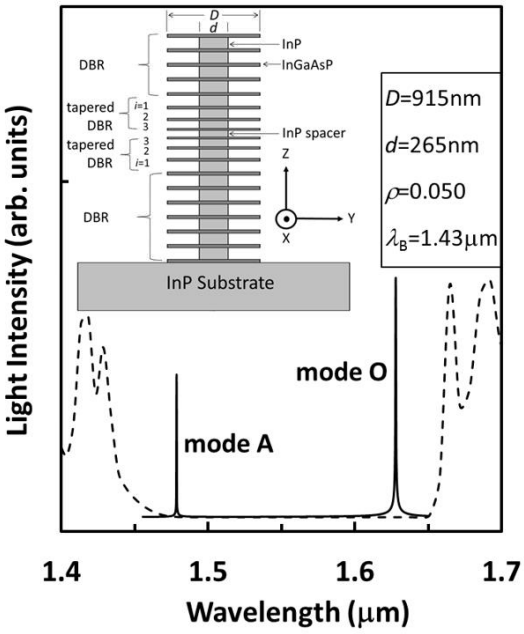

FIG. 1. An example of the calculated optical mode spectra (solid line) of the InGaAsP/InP-air-aperture micropillar cavities, with the stopband shown by a dashed line. The upper inset is the schematic diagram of the YZ cross-section of an ideal InGaAsP/InP-air-aperture micropillar cavity.

The cavity characters are calculated by running the numerical simulation tool Rsoft, which is based on a finite-difference time-domain method. By launching a polarized impulse from the light source, the time evolution of the light field can be obtained in the whole cavity. Taking the time-dependent light field at a typical point, Fourier transform gives a spectrum showing the existing optical modes appearing at some wavelengths. By setting the light source as a narrowband emission around a mode wavelength λ, simulation gives the light intensity decaying with time t and the steady state light field distribution, i.e., the mode profile. The quality factor Q is obtained by fitting the exponential light intensity envelope to $\exp(-2\pi ct/Q\lambda)$, where c is the light velocity in vacuum. The mode volume V (in unit of $(\lambda/n)^3$ where n is the refractive index of the layer of maximum light intensity) is gotten by integrating the light intensity over the cavity and normalizing it to the maximum light intensity point. The optical stopband, within which the optical modes must locate, is obtained by calculating the DBRs with a light source set outside the top surface.

High quality can be obtained when the cavity has 4 (6.5) pairs of InGaAsP/InP-air-aperture layers in the top (bottom) DBRs and $N = 3$ segments of InGaAsP/InP-air-aperture layers in the tapered DBRs. A typical calculated optical mode spectrum is shown in Fig. 1. There are often two good optical modes, mode O and mode A, simultaneously existing in such cavities [12]. As the lowest two modes of the cavity, they are probably formed by mode coupling between two fundamental modes corresponding to two differently sized micropillars, since the cavity looks like a mixture of two different micropillars. As a result of mode mixing, the lower mode O has symmetric profile, but the upper mode A has antisymmetric profile along the Z direction. What is more important, the two modes can be individually optimized by tuning the cavity structure. When the outer diameter $D_o = 915$ nm, inner diameter $d_o = 265$ nm, $\lambda_B = 1.40$ μm, and $\rho = 0.065$, the fundamental cavity mode (mode O) peaks at $\lambda = 1.55$ μm with the quality factor $Q_o = 1.5 \times 10^4$. Tuning $D_o = 935$ nm, $d_o = 260$ nm, $\lambda_B = 1.46$ μm and $\rho = 0.04$, an optimized mode A appears at $\lambda = 1.55$

μm with the quality factor $Q_o = 1.3 \times 10^5$. The mode volume of these two optimized modes are $V \sim 1$ in terms of $(\lambda/n)^3$. These ideal cavities can be expected to serve as efficient and even coherent 1.55-μm QD SPS since their modes O and A well satisfy the weak and strong coupling to the QD emitter, respectively [12].

III. UNCERTAINTY MODELS AND SIMULATION RESULTS

A typical fabrication process of InGaAsP/InP-air-aperture micropillar cavities includes 3 steps. First, epitaxial growth, e.g., molecular beam epitaxy or metalorganic chemical vapor deposition, is used to form an InP/InGaAsP multilayer structure on an InP substrate. Next, InP/InGaAsP micropillars are formed by mask-protectively dry-etching the epitaxial multilayers down to the InP substrate using processing such as induction coupled plasma etching or reactive ion etching. Finally, InP layers in the micropillar are partially removed by wet-chemically etching through the pillar's side edges to form air-apertures. Although simple and monolithic, and as is more advantageous than the process for hybrid cavities [9-11], such a presently imperfect process must introduce fabrication errors which influence the cavity quality. The precision of the epitaxial growth technique is responsible for the uniformity of layer thickness. The dry- and wet-etching effects are usually material, depth, reactive gas, and reaction-product dependent, so they might cause shape distortion, fluctuating layer diameter and surface roughness.

To clarify whether and how an imperfect InGaAsP/InP-air-aperture micropillar cavity serves as useful 1.55-μm QD SPS, we investigate here the cavity quality depending on the layer size fluctuation, sidewall surface roughness and cavity shape change. Before that study, we need to make clear the criteria for quantitatively judging the influence of imperfect fabrication. Applying the cavity quantum electrodynamics theory [15] and considering the property of InAs/InP QDs [16], it was shown that Q/V over 3000 can realize a weakly coupling cavity with Purcell factor of more than 100 [12], which improves the 1.55-μm QD SPS to be GHz bright and photon-indistinguishable. Similarly, coherent operation of a 1.55-μm QD SPS, requiring strong coupling between the QD emitter and the cavity mode, can be well satisfied by setting $Q/\sqrt{V}$ more than 10^4 [12]. Considering $V \sim 1$ for these cavities, $Q > 3000$ and $Q > 10000$ will be taken to be the criteria for an efficient and a coherent 1.55-μm QD SPS, respectively.

3.1. Tolerance on Layer Size Fluctuation

The thickness and diameter of the layers in an InGaAsP/InP-air-aperture micropillar cavity are usually fluctuating after fabrication. We randomly set the thickness of different layers changing as $t = t_o + \alpha\Delta t$, and the diameter of different layer disks changing as $D = D_o + \alpha\Delta D$, $d = d_o + \alpha\Delta d$, where t_o, D_o, d_o are the originally optimized sizes, Δt (ΔD, Δd) is the standard deviation of the thickness (diameter) distribution, and α is a random value following a normal distribution with average of 0 and standard deviation of 1. In this work, we usually set $\Delta D = \Delta d$ unless specifically stated. The InGaAs/InP-air-aperture micropillar cavity structure with layer thickness and diameter fluctuations is schematically demonstrated by the upper inset of Fig. 2. In brief, the layer thickness (diameter) of the imperfect cavity follows a normal distribution with $t = t_o \pm \Delta t$ and/or $D = D_o \pm \Delta d$ and $d = d_o \pm \Delta d$.

At first, let us see the effect with only fluctuating layer thickness. As indicated by the data points around 0 nm in Fig. 2, fluctuation in thickness degrades Q factor and distributes it into a larger range. In detail, as the thickness fluctuates with standard deviation of 2% (5%), i.e. $\Delta t/t_o$ = 2% (5%), the Q factor of mode A degrades from 1.3×10^5 to $0.6 - 1.1 \times 10^5$ ($2.0 - 4.8 \times 10^4$), while that of mode O changes from 1.5×10^4 to $0.9 - 1.4 \times 10^4$ ($0.4 - 1.3 \times 10^4$). Fluctuation only in layer diameter also degrades the cavity quality. As shown by the cross symbols in Fig. 2, when the standard deviation of D and d comes up to 5.3 (13.3) nm, i.e. $\Delta D = \Delta d = 5.3$ (13.3) nm, the Q factor of mode A distributes in a range of $0.8 - 1.1 \times 10^5$ ($2.5 - 7.0 \times 10^4$); while that of mode O slightly changes to $1.2 - 1.3 \times 10^4$ ($0.9 - 1.3 \times 10^4$). Referring to the criteria $Q > 3000$ (mode

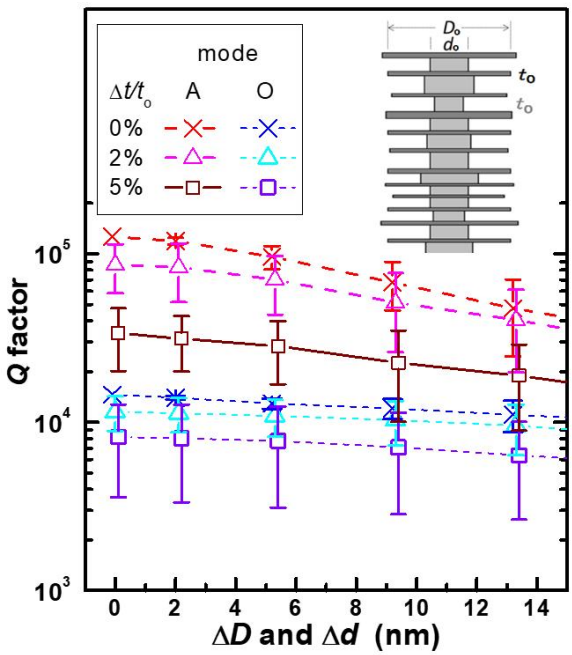

FIG. 2. The Q factor as a function of cavity layer diameter variation ΔD and Δd together with the layer thickness fluctuation Δt for the modes A and O of the InGaAsP/InP-air-aperture micropillar cavities. The upper right inset is the schematic cavity model showing the variation of layer thickness and diameters. For clear display, part of the data points are slightly shifted.

O) and $Q > 10000$ (mode A), it suggests that the cavity can tolerate fluctuation of at least ±2% in layer thickness or at least ±5 nm in layer diameter.

To approach the real fabrication condition, we set simultaneously the variations of diameters and thicknesses of the cavity layers in the following. With a fixed thickness fluctuation degree, the increasing diameter fluctuation leads to a slow but obvious degradation in mode A and almost no degradation in mode O. For examples, together with 2% of thickness fluctuation, 5.3 (13.3) nm of diameter variation results in Q factor of mode A changing from 0.6 - 1.1 × 10^5 to 0.4 - 1.0 × 10^5 (2.5 - 6.0 × 10^4), and that of mode O changing from 0.9 - 1.4 × 10^4 to 0.8 - 1.3 × 10^4 (0.6 - 1.2 × 10^4); with 5% of thickness fluctuation, it gives Q factor of mode A changing from 2.0 - 4.8 × 10^4 to 1.7 - 4.0 × 10^4 (0.9 - 2.9 × 10^4), and that of mode O changing from 0.4 - 1.3 × 10^4 to 0.3 - 1.2 × 10^4 (0.3 - 1.0 × 10^4). In average, ±2% of thickness fluctuation and ±5 nm of diameter fluctuation result in Q factor more than 7 × 10^4 (1 × 10^4) in mode A (O), with which the high quality of the cavity remains; whereas ±5% of thickness and ±13 nm of diameter fluctuations lead to Q factor above 2 × 10^4 (6 × 10^3) for mode A (O), with which the micropillar cavity is still useful. Together with the fact that the mode wavelength varies within ±15 nm and the mode volume changes within ±2% in the above processing error range (not shown), it suggests that our cavities tolerate layer thickness uncertainty at least ±2% and layer diameter variation at least ±5 nm.

The different Q degradations in two modes may be comprehended as follows. Any processing uncertainty causes actually more optical loss $1/Q_p$, and the total loss is thus $1/Q = 1/Q_o + 1/Q_p$. The same degree of processing uncertainty leads to roughly the same Q_p to both modes O and A. With a Q_p much higher than Q_o of mode O (~10^4) but comparable to Q_o of mode A (~10^5), the reduced Q can exhibit almost no degrading for mode O but obvious decreasing for mode A. It means that the effect of processing uncertainty might be much weaker than the original loss mechanism of mode O but in the same order of magnitude as that of mode A, suggesting the relatively high processing robustness of the proposed InGaAsP/InP-air-aperture micropillar cavities.

The combined effect, especially for small fabrication uncertainty, is seen roughly following $Q_{td}/Q_o = Q_tQ_d/Q_o^2$, where Q_{td} is the average quality factor with both thickness and diameter changes, Q_t (Q_d) is that with only change in layer thickness (diameter). For examples, the mode A under ±2% (±5%) of thickness fluctuation has $Q_t/Q_o = 8.7 \times 10^4$ (2.8×10^4) / $1.3 \times 10^5 = 0.67$ (0.22), and that under ±5 nm of diameter variation shows $Q_d/Q_o = 9.6 \times 10^4 / 1.3 \times 10^5 =$ 0.74, so with the condition of ±2% (±5%) thickness together with ±5 nm diameter fluctuations, the quality factor of mode A can be estimated being $Q_{td} = 0.67$ (0.22) × 0.74 × $Q_o = 6.4 \times 10^4$ (2.4×10^4), which is close to the simulated average value 7.0 × 10^4 (2.8 × 10^4). This empirical estimation helps the discussion later in this work.

3.2. Tolerance on Sidewall Surface Roughness

The real processing could also lead to imperfect surface morphology [14]. It is thus necessary to study the effect of sidewall surface roughness on the InGaAsP/InP-air-aperture micropillar cavity. The processing induced sidewall surface roughness is modeled in two types. In type I, as schematically shown by the upper-left inset of Fig. 3, we replace the circular circumference with a polygon of 66 random sides, where the distance between a vertex and the original disk center R (r) follows a normal distribution $R_o \pm 1.5\Delta R$ ($r_o \pm 1.5\Delta r$) and the side length changes following a normal distribution (1 ± 20%) $2\pi R_o/66$. In type II, there set about 50 small bulges and pits iterated on the side surface of a layer, whose height /depth and open angle are randomly and normally distributed as $R_o \pm 2\Delta R$ ($r_o \pm 2\Delta r$) and 40° ± 20°, respectively. This model is schematically shown by the upper-right inset of Fig. 3. By integrating over the whole side surface, it is found that the sidewall surface roughness RMS is close to ΔR (Δr) in the above both types, so we use the data of preset ΔR (Δr) to represent the average sidewall surface roughness. Considering that the InP layer is about three times thicker than InGaAsP layer, each InP layer is divided into three layers to set three different sets of surface roughness data. Furthermore, in one calculation trial, the roughness percentages of the big InGaAsP and small InP layers are set to be the same, i.e., $\Delta R/R_o = \Delta r/r_o$.

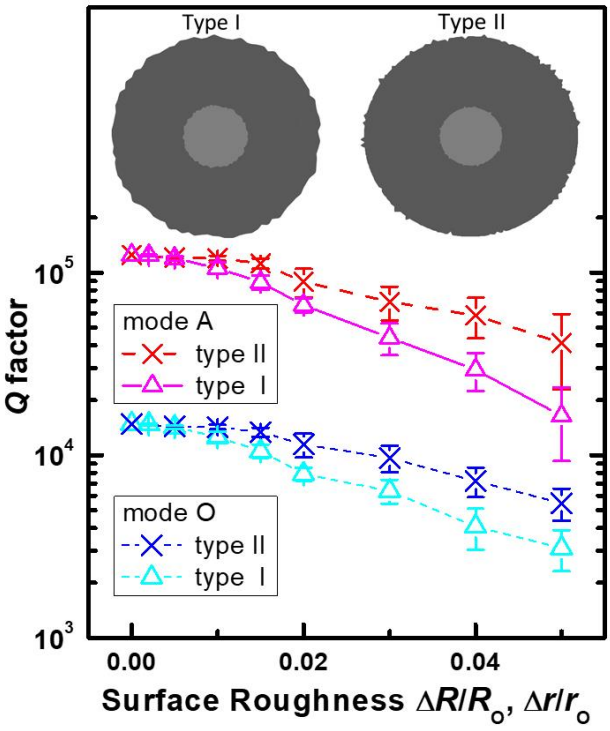

FIG. 3. The calculated Q factors as functions of the sidewall surface roughness for the modes A and O of the InGaAsP/InP-air-aperture micropillar cavities. The upper insets are the schematic XY cross-sections of the modeled cavities, showing the surface roughness set in two types.

From the results shown in Fig. 3, we see that the sidewall surface roughness could affect the Q factor of the InGaAsP/InP-air-aperture micropillar cavity. Up to 1% of $\Delta R/R_o$ and $\Delta r/r_o$, the Q factor slightly degrades to above 80% of the ideal value, e.g. 1.2×10^5 (type II) / 1.05×10^5 (type I) for mode A, and 1.4×10^4 (type II) / 1.25×10^4 (type I) for mode O. With sidewall surface roughness $\Delta R/R_o = \Delta r/r_o = 2\%$, the Q factor degrades to 0.7 - 1.0 $\times 10^5$ (type II) / 0.6 - 0.7 $\times 10^5$ (type I) for mode A, and 0.9 - 1.2 $\times 10^4$ (type II) / 0.7 - 0.8 $\times 10^4$ (type I) for mode O, which are still close to the ideal values. With 5% of surface roughness, the Q factor is significantly degraded to 2 - 6 $\times 10^4$ (type II) / 1 - 2 $\times 10^4$ (type I) for mode A, and 4 - 6 $\times 10^3$ (type II) / 1 - 3 $\times 10^3$ (type I) for mode O, which are approaching the critical values of a useful cavity. At the same time, the mode wavelength remains 1.55 ± 0.01 μm and the mode volume changes by as little as ±1% in the above range of surface roughness (not shown). Referring to the criteria $Q > 3000$ (mode O) and $Q > 10000$ (mode A), we could say that the surface roughness tolerance of the InGaAsP/InP-air-aperture micropillar cavity is at least ±2% of the layer radii, i.e., about ±2.5 nm on the small InP and ±20 nm on the larger InGaAsP layers' side-surfaces.

3.3. Tolerance on Cavity Shape Change

Considering a real micropillar cavity out of shape, which may result from using an etch mask not sufficiently resistive in fabrication [17], we shall now study the effect of imperfect cavity shape. We use a truncated cone to approximate this imperfection, i.e., declining the outer and/or inner sidewall of our cavity pillar to some degree of angle away from the straightly vertical direction while remaining the central XY plane of the spacer (central) layer unchanged. The model is schematically shown by the inset of Fig. 4, although, for clarity, only the lower part is displayed.

The result of truncated-cone shaped InGaAsP/InP-air-aperture micropillar cavity is shown in Fig. 4. In the case $\theta = 3\theta_i$, where θ and θ_i are the tilt angles of the outer and inner sidewalls respectively, the Q factor sounds quite subject to cone-shape change in the cavity. It degrades for almost two orders of magnitude as the sidewall angle goes to more than 2º, because the top and bottom layers have diameters ~300 nm (outer) and ~70 nm (inner) different from the central layers. However, if the cavity shape is not much changed, the Q factors can remain above a value high enough. The mode A can be more than 4×10^4, and the mode O can be more than 3×10^3 as the sidewall angle θ keeps smaller than 1.5º, in which case the top and bottom layers have diameters ~160 nm (outer) and ~40 nm (inner) different from the central layers. Very close change of Q factor can be seen in the case of $\theta_i = 0$, i.e., when the inner layers maintain the optimized cylinder and only the outer sidewall tilts. In the case $\theta = \theta_i$, where the outer and inner sidewalls tilt in the same way, the Q factors of both modes O and A decrease in even faster rates than

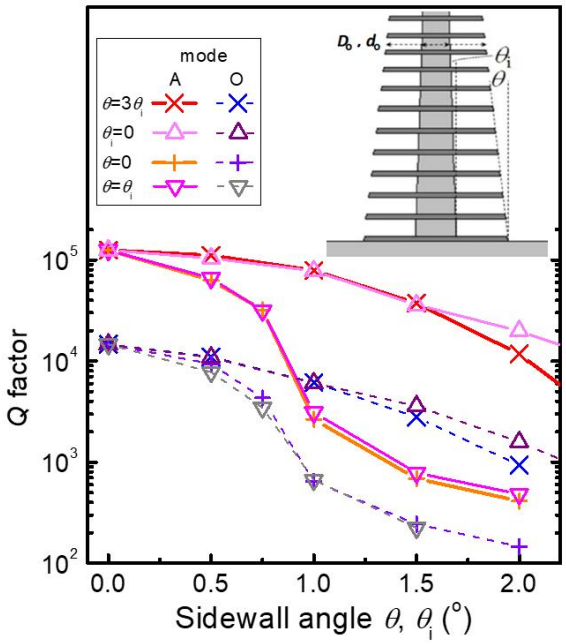

FIG. 4. The Q factors of the truncated-cone shaped InGaAsP/InP-air-aperture micropillar cavities as functions of the sidewall angle for both modes O and A. The upper-right inset is the schematic diagram of partial vertical cross section of a truncated-cone shaped cavity.

those in the case $\theta = 3\theta_i$. The case with $\theta = 0$, i.e., where the outer layers hold the optimized cylinder and only the inner sidewall tilts, behaves in nearly the same way. In detail, the Q factors of both modes A and O first degrade slowly to about $Q_o/4$ (at θ_i of 0.7°) and then drop significantly by more than one order of magnitude. The result is similar if the side angle is negative, i.e., when the cavity shape shows larger diameters on the top and smaller diameters on the bottom sides. In addition, the wavelength and mode volume do not vary much in the above range of the cavity shape change. These results suggest that the inner sidewall dominates the effect of cavity shape change. At the same time, the far field pattern is found remaining a Gaussian shape but increasing in divergence by less than 10% (θ, $\theta_i \sim 0.5°$) - 20% (θ, $\theta_i > 1.5°$). Thus the collection efficiency into optical fiber would not be significantly degraded by cavity sidewall declining within the studied range. By seeing the results related to the inner sidewall inclination angle, we may state that the InGaAsP/InP-air-aperture micropillar cavity can tolerate a shape change with 0.7° sidewall tilt.

IV. DISCUSSION

In the above, we have studied the fabrication tolerance individually to layer size uncertainty, sidewall surface roughness and shape distortion of the InGaAsP/InP-air-aperture micropillar cavities. Refer to the approximated

characterization on the effect of simultaneous thickness and diameter fluctuations, the combined effect of all the layer size, sidewall surface and shape imperfections can be estimated. From the simulated data, with only $\Delta t = 2\% / \Delta d = 5$ nm, the average quality factor $Q_{td} = 7.1 \times 10^4$ (mode A), 1.1×10^4 (mode O); with only surface roughness $\Delta R/R_o = \Delta r/r_o = 1.5\%$, it is $Q_r = 8.9 \times 10^5$ (mode A), 9.8×10^3 (mode O); with only sidewall inclination $\theta = \theta_I = 0.5°$, it is $Q_\theta = 6.9 \times 10^4$ (mode A), 7.3×10^3 (mode O). With all the above imperfections existing together, the Q factor can be estimated $Q_{tdr\theta} = Q_{td}Q_rQ_\theta/Q_o^2 = 2.6 \times 10^4$ (mode A), 3.5×10^3 (mode O). It thus gives a fabrication tolerance of our cavity, ±2% in layer thickness, ±5 nm in diameter, ±2.5 nm in sidewall surface roughness and 0.5° in sidewall inclination.

Then, let us check whether the above tolerated processing conditions are feasible in practice. First, it is easy to reach a thickness precision better than ±2% (about ±2 nm) in DBR-like multilayer structure growth [18], because the well-developed epitaxial technique has been able to control layer thickness at a level of monolayer accuracy. General photolithography is still challenging to achieve a sub-micrometer-scale accuracy and nano-scaled surface roughness. However, using the advanced micro-/nano-processing techniques, a semiconductor pillar-like structure can be controlled to have diameter uncertainty as small as ±2% or ±5 nm [19, 20] and sidewall inclination as small as 0.5° [21], although both of them are not so easy. It has been reported that advanced techniques allow controlling sidewall surface roughness of InP-based nanostructures to be less than 1 nm [22], thus the sidewall surface roughness tolerance of ±2.5 nm can be technically satisfied in fabrication processing. It turns out that the fabrication tolerance of the InGaAsP/InP-air-aperture micropillar cavities is practically reachable.

From the above study, it is clear that the mode O can keep Q/V more than 3500 under the accessible processing precisions, and remain it as high as 10^4 under well-controlled processing conditions. It is thus suggestive of the robustness against fabrication conditions of the InGaAsP/InP-air-aperture micropillar cavities as efficient QD SPSs at 1.55 μm. The mode A satisfies $Q/\sqrt{V} \geq 2.6 \times 10^4$ under the currently available fabrication precisions, so it can be expected to practically realize a coherent 1.55-μm QD SPS. Therefore, the proposed InGaAsP/InP-air-aperture micropillar cavities are confirmed achievable as highly effective quantum devices to be applied in silica-fiber-based quantum networks.

V. CONCLUSION

To summarize, with proper models, we investigate the fabrication tolerance of InGaAsP/InP-air-aperture micropillar cavities as the candidates of 1.55-μm QD SPSs. Simulations show that, the Q factor of the cavities can be kept high enough for efficient and coherent QD SPSs when the fabrication condition satisfies layer thickness uncertainty of ±2% (~±2 nm), diameter variation of ±5 nm, side surface roughness of ±5 nm and sidewall inclination of 0.5°. The above tolerance levels are all practically available in presently advanced fabrication techniques, so the InGaAsP/InP-air-aperture micropillar cavities are hopefully feasible to be applied in silica-fiber based quantum information networks.

ACKNOWLEDGMENT

This study was supported by a grant from the Sichuan Science and Technology Program [grant number 2018JY 0084], the 1000 Talents Plan of Sichuan Province, and the Rongpiao Plan of Chengdu City.

REFERENCES

1. P. Michler, A. Kiraz, C. Becher, W. V. Schoenfeld, P. M. Petroff, L. Zhang, E. Hu, and A. Imamoğlu, "A quantum dot single-photon turnstile device," Science **290**, 2282-2285 (2000).
2. C. Santori, D. Fattal, J. Vučković, G. S. Solomon, and Y. Yamamoto, "Indistinguishable photons from a single-photon device," Nature **419**, 594-597 (2002).
3. O. Gazzano, S. M. de Vasconcellos, C. Arnold, A. Nowak, E. Galopin, I. Sagnes, L. Lanco, A. Lemaître, and P. Senellart, "Bright solid-state sources of indistinguishable single photons," Nat. Commun. **4**, 1425 (2013).
4. M. Nomura, N. Kumagai, S. Iwamoto, Y. Ota, and Y. Arakawa, "Laser oscillation in a strongly coupled single-quantum-dot-nanocavity system," Nat. Phys. **6**, 279-283 (2010).
5. M. Pelton, J. Vučković, G. S. Solomon, A. Scherer, and Y. Yamamoto, "Three-dimensionally confined modes in micropost microcavities: quality factors and Purcell factors," IEEE J. Quantum Electron. **38**, 170-177 (2002).
6. A. Faraon, I. Fushman, D. Englund, N. Stoltz, P. M. Petroff, and J. Vučković, "Coherent generation of non-classical light on a chip via photon-induced tunnelling and blockade," Nat. Phys. **4**, 859-863 (2008).
7. K. Takemoto, Y. Nambu, T. Miyazawa, Y. Sakuma, T. Yamamoto, S. Yorozu, and Y. Arakawa, "Quantum key distribution over 120 km using ultrahigh purity single-photon source and superconducting single-photon detectors," Sci. Rep. **5**, 14383 (2015).
8. C.-K. Lin, D. P. Bour, J. Zhu, W. H. Perez, M. H. Leary, A. Tandon, S. W. Corzine, and M. R. T. Tan, "High temperature continuous-wave operation of 1.3- and 1.55-μm VCSELs with InP/air-gap DBRs," IEEE J. Sel. Top. Quantum Electron. **9**, 1415-1421 (2003).
9. D. Dalacu, D. Poitras, J. Lefebvre, P. J. Poole, G. C. Aers, and R. L. Williams, "InAs/InP quantum-dot pillar microcavities using SiO_2/Ta_2O_5 Bragg reflectors with emission around 1.55 μm," Appl. Phys. Lett. **84**, 3235 (2004).
10. H.-Z. Song, K. Takemoto, T. Miyazawa, M. Takatsu, S.

Iwamoto, T. Yamamoto, and Y. Arakawa, "Design of Si/SiO_2 micropillar cavities for Purcell-enhanced single photon emission at 1.55 μm from InAs/InP quantum dots," Opt. Lett. **38**, 3241-3244 (2013).
11. H.-Z. Song, K. Takemoto, T. Miyazawa, M. Takatsu, S. Iwamoto, M. Ekawa, T. Yamamoto, and Y. Arakawa, "High quality-factor Si/SiO_2-InP hybrid micropillar cavities with submicrometer diameter for 1.55-μm telecommunication band," Opt. Express **23**, 16264-16272 (2015).
12. H.-Z. Song, M. Hadi, Y. Zheng, B. Shen, L. Zhang, Z. Ren, R. Gao, and Z. M. Wang, "InGaAsP/InP nanocavity for single-photon source at 1.55-μm telecommunication band," Nanoscale Res. Lett. **12**, 128 (2017).
13. J. Gessler, T. Steinl, A. Mika, J. Fischer, G. Sek, J. Misiewicz, S. Höfling, C. Schneider, and M. Kamp, "Low dimensional GaAs/air vertical microcavity lasers," Appl. Phys. Lett. **104**, 081113 (2014).
14. A. J. Shields, "Semiconductor quantum light sources," Nat. Photon. **1**, 215-223 (2007).
15. A. Auffèves, D. Gerace, J.-M. Gérard, M. F. Santos, L. C. Andreani, and J.-P. Poizat, "Controlling the dynamics of a coupled atom-cavity system by pure dephasing," Phys. Rev. B **81**, 245419 (2010).
16. T. Kuroda, Y. Sakuma, K. Sakoda, K. Takemoto, and T. Usuki, "Decoherence of single photons from an InAs/InP quantum dot emitting at a 1.3 μm wavelength," Phys. Stat. Sol. C **6**, 944-947 (2009).
17. S. Bouchoule, G. Patriarche, S. Guilet, L. Gatilova, L. Largeau, and P. Chabert, "Sidewall passivation assisted by a silicon coverplate during Cl_2-H_2 and HBr inductively coupled plasma etching of InP for photonic devices," J. Vac. Sci. Technol. B **26**, 666 (2008).
18. A. S. Kurochkin, I. I. Novikov, L. Ya Karachinsky, D. V. Denisov, A. G. Gladyshev, G. A. Gusev, A. N. Sofronov, A. A. Usikova, Yu M. Zadiranov, G. S. Sokolovsky, V. M. Ustinov, and A. Yu Egorov, "MBE growth and characterization of InAlAs/InGaAs 9 μm range quantum cascade laser," J. Phys.: Conf. Ser. **917**, 052016 (2017).
19. T. Heuser, J. Große, A. Kaganskiy, D. Brunner, and S. Reitzenstein, "Fabrication of dense diameter-tuned quantum dot micropillar arrays for applications in photonic information processing," APL Photonics **3**, 116103 (2018).
20. D. M. Beggs, L. O'Faolain, and T. F. Krauss, "Accurate determination of the functional hole size in photonic crystal slabs using optical methods," Photonics Nanostruc. **6**, 213-218 (2008).
21. J. S. Parker, E. J. Norberg, R. S. Guzzon, S. C. Nicholes, and L. A. Coldren, "High verticality InP/InGaAsP etching in $Cl_2/H_2/Ar$ inductively coupled plasma for photonic integrated circuits," J. Vac. Sci. Technol. B **29**, 011016 (2011).
22. B. Rong, E. van der Drift, R. W. van der Heijden, and H. W. M. Salemink, "2D InP photonic crystal fabrication process development," Proc. SPIE **6327**, 632715 (2006).